AD-A081 011 ARMY MISSILE COMMAND REDSTONE ARSENAL AL GROUND EQU--ETC F/G 20/1
A THERMOPLASTIC DEVICE FOR REAL-TIME IN SITU RECORDING OF ACOUS--ETC(U)
OCT 79 H LIU
UNCLASSIFIED DRSMI/RL-80-4 NL

| OF |
AD
A081011

END
DATE FILMED
3-80
DDC

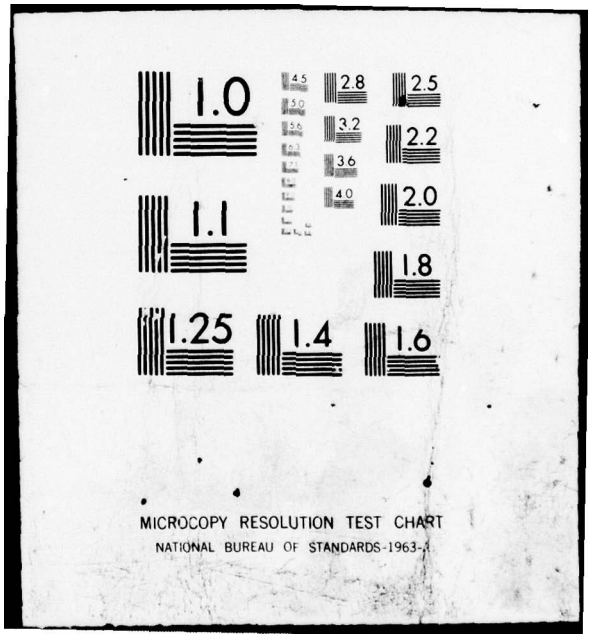
1.0
1.1
1.25
1.4
1.6
1.8
2.0
2.2
2.5
2.8
3.2
3.6
4.0
4.5
5.0
5.6
MICROCOPY RESOLUTION TEST CHART
NATIONAL BUREAU OF STANDARDS-1963-A

TECHNICAL REPORT RL-80-4

# A THERMOPLASTIC DEVICE FOR REAL-TIME *IN SITU* RECORDING OF ACOUSTICAL HOLOGRAMS

Hua-Kuang Liu
Department of Electrical Engineering
University of Alabama
University, Alabama 35486

for

Ground Equipment and Missile Structures Directorate
US Army Missile Laboratory



1 October 1979

U.S. ARMY MISSILE COMMAND
Redstone Arsenal, Alabama 35809

**DISPOSITION INSTRUCTIONS**

DESTROY THIS REPORT WHEN IT IS NO LONGER NEEDED. DO NOT RETURN IT TO THE ORIGINATOR.

**DISCLAIMER**

THE FINDINGS IN THIS REPORT ARE NOT TO BE CONSTRUED AS AN OFFICIAL DEPARTMENT OF THE ARMY POSITION UNLESS SO DESIGNATED BY OTHER AUTHORIZED DOCUMENTS.

**TRADE NAMES**

USE OF TRADE NAMES OR MANUFACTURERS IN THIS REPORT DOES NOT CONSTITUTE AN OFFICIAL ENDORSEMENT OR APPROVAL OF THE USE OF SUCH COMMERCIAL HARDWARE OR SOFTWARE.

Unclassified

SECURITY CLASSIFICATION OF THIS PAGE (When Data Entered)

| REPORT DOCUMENTATION PAGE | READ INSTRUCTIONS BEFORE COMPLETING FORM |
|---|---|
| 1. REPORT NUMBER: RL-80-4 | 2. GOVT ACCESSION NO. |
| 3. RECIPIENT'S CATALOG NUMBER: 9 | |
| 4. TITLE (and Subtitle): A THERMOPLASTIC DEVICE FOR REAL-TIME IN SITU RECORDING OF ACOUSTICAL HOLOGRAMS. | 5. TYPE OF REPORT & PERIOD COVERED: Technical Report |
| | 6. PERFORMING ORG. REPORT NUMBER |
| 7. AUTHOR(s): Hua-Kuang Liu, University of Alabama | 8. CONTRACT OR GRANT NUMBER(s) |
| 9. PERFORMING ORGANIZATION NAME AND ADDRESS: Commander, US Army Missile Command, ATTN: DRSMI-RLA, Redstone Arsenal, Alabama 35809 | 10. PROGRAM ELEMENT, PROJECT, TASK AREA & WORK UNIT NUMBERS: 12 45 |
| 11. CONTROLLING OFFICE NAME AND ADDRESS: Commander, US Army Missile Command, ATTN: DRSMI-RPT, Redstone Arsenal, Alabama 35809 | 12. REPORT DATE: 1 October 1979 |
| | 13. NUMBER OF PAGES: 50 |
| 14. MONITORING AGENCY NAME & ADDRESS(if different from Controlling Office): DRSMI/RL-80-4 | 15. SECURITY CLASS. (of this report): Unclassified |
| | 15a. DECLASSIFICATION/DOWNGRADING SCHEDULE |

16. DISTRIBUTION STATEMENT (of this Report)

Approved for public release; distribution unlimited.

17. DISTRIBUTION STATEMENT (of the abstract entered in Block 20, if different from Report)

18. SUPPLEMENTARY NOTES

This report was accomplished through the Laboratory Research Cooperative Program (LRCP) between Dr Hua-Kuang Liu of the Department of Electrical Engineering, University of Alabama, and the US Army Missile Command.

19. KEY WORDS (Continue on reverse side if necessary and identify by block number)

Real Time Acoustical Holography
Thermoplastic
Optical Reconstruction
Flaw Detection and Quantification
Nondestructive Testing

20. ABSTRACT (Continue on reverse side if necessary and identify by block number)

Theory and experimental results of a thermoplastic device for real-time in situ acoustical holographic recording are presented. The theoretical analysis takes the possible existence of an in-line reference beam and its influence on the real-time coherent optical image reconstruction into consideration. A new technique has been used for fabricating the thermoplastic devices. The preliminary experimental data have demonstrated the feasibility of the application of the device for recordings of acoustical holograms.

DD FORM 1 JAN 73 1473 EDITION OF 1 NOV 65 IS OBSOLETE

Unclassified

SECURITY CLASSIFICATION OF THIS PAGE (When Data Entered)

## ACKNOWLEDGMENT

The author deeply appreciates the valuable discussions and collabórations with Dr. William F. Swinson of Auburn University and Mr. John A. Schaeffel of the US Army Missile Command in carrying out this project. He would also like to thank Mr. Terry L. Vandiver, Mr. Robert B. McGowan, Mrs. Alison Demsey, and Mr. Keith Rogers for their technical assistances in the fabrication of the device. In addition, helpful suggestions by Drs. J. E. Wolfe, N. C. Stewart, and L. S. Cosentino, and free thermoplastic samples generously given by Hercules Inc. of Wilmington, Delaware are highly appreciated.

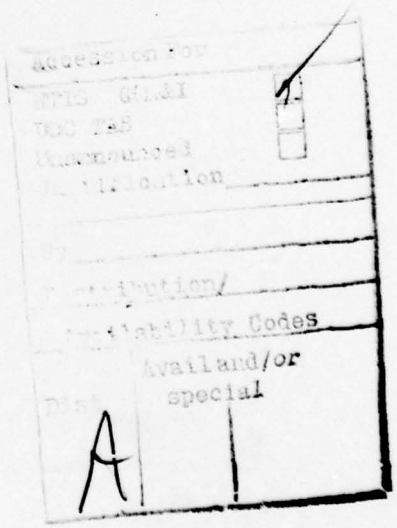

# CONTENTS

# ILLUSTRATIONS

## ILLUSTRATIONS (Concluded)

# I. INTRODUCTION

Deformable thermoplastic material has been used with considerable success in *in Situ* optical holographic recordings. [1-22] Advantages of a device made of this material include the fact that the device has the capability of near real-time holographic reconstruction, it can be recycled, wet processed and dark-room handling can be eliminated. Resolution in excess of 4000 cycles per millimeter can be achieved. Nevertheless, it seems that the material has received very little attention on its potentiality of being used for the recording of acoustical holograms after the idea was first introduced by Young and Wolfe [23] in 1967. In this report, a detailed theoretical analysis and some preliminary experimental results of a thermoplastic acoustical holographic recording devices will be presented. The work is different from that reported by Young and Wolfe in two major regards:

(1) The recording area of the device is 50 times or larger than their device.

(2) Optical holographic image reconstruction process is in real-time and *in situ*.

Section II is a theoretical analysis of the device, and the experiment and discussion are presented in Sections III and IV, respectively.

# II. THEORY

The theoretical analysis of the holographic recording of the thermoplastic device is divided into two parts.

The first part is a description of the interaction of the ultrasound with the liquefied thermoplastic surface. The second part deals with the principle of image reconstruction by laser light. The analysis is similar in the basic approach adopted by Brenden [24] but is different from his model for the fact that the existence of an auxiliary reference wave which originated from the object beam transducer is considered. This additional reference beam exists because of the simplicity of the geometry of the test objects in some cases. The assumption will make mathematical analysis more tedious but is nevertheless necessary due to the requirement of the interpretation of the experimental results.

In the second part, the process of coherent optical image reconstruction of the acoustical hologram is described.

## A. Interaction of Ultrasound With the Liquefied Thermoplastic Surface

In the acoustical holographic system as shown in *Figure 1*, the reference beam is with amplitude $A_r$, generated by the reference transducer is incident upon the surface ($z = 0$) of the thermoplastic layer at an angle $\Theta_r$, while the object beam with amplitude $A_{ob}$ is incident at an angle $\Phi_o$ with respect to the perpendicular of the surface and carries an object-dependent phase $\phi(x,y)$. If the object is simple, such as a coarse grating structure, part of the beam generated by the object transducer may traverse through the object plane without being modulated by the object. The portion of the beam with amplitude $A_o$ and incident angle $\Theta_o$ may be considered in essence a reference beam for the hologram. These waves are listed below:

$$\text{Reference beam No. 1:} \quad R_1 = A_r \exp(j\, k_r\, y) \tag{1}$$

$$\text{Object beam:} \quad O = A_{ob} \exp[-j(k_o y + \phi(x,y))] \tag{2}$$

$$\text{Reference beam No. 2:} \quad R_2 = A_o \exp(-j\, k_o\, y) \tag{3}$$

where

$$k_r = \frac{2\pi}{\lambda} \sin\Theta_r, \text{ and } k_o = \frac{2\pi}{\lambda} \sin\Theta_o \ , \tag{4}$$

and $\lambda$ is the wavelength of the acoustic wave.

Simultaneous presence of these waves and the change of momentum on reflection at the surface produces a radiation pressure given by

$$p(x,y) = |O + R_1 + R_2|^2 / (\rho\, v_s^2) \tag{5}$$

where $\rho$ is the density of the thermoplastic and $v_s$ is the velocity of sound.

The radiation pressure is counterbalanced by gravity, $\rho gZ$, and surface tension

$$p_t = - c_s \left( \frac{\partial^2 z}{\partial x^2} + \frac{\partial^2 z}{\partial y^2} \right) \ , \tag{6}$$

where $c_s$ is the surface tension coefficient. For a unit area, the balance of force equation is

$$p(x,y) = \rho g z - c_s \left( \frac{\partial^2 z}{\partial x^2} + \frac{\partial^2 z}{\partial y^2} \right) \ . \tag{7}$$

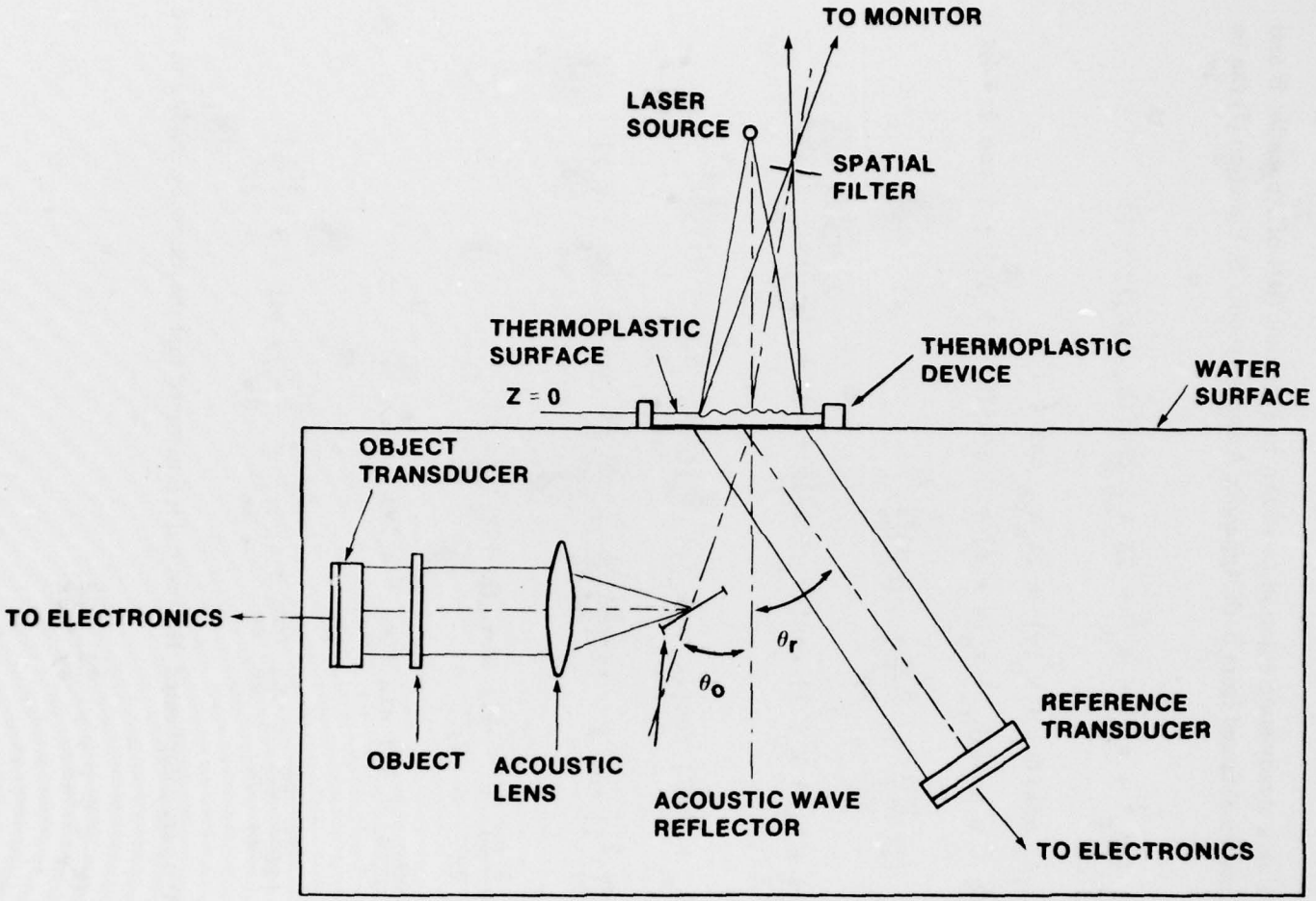


**Figure 1. The thermoplastic acoustical holographic recording system with *in situ* real-time optical image reconstruction.**

Solution of the above equation for $z$ yields the displacement of the thermoplastic surface.

Assuming a steady-state solution as shown in Equation (B1) of Appendix B and applying the results obtained from both Appendix A and Appendix B, Equation (7) can be rewritten as

$$\frac{1}{\rho v_s^2}\{A_r^2 + A_{ob}^2 + A_o^2 + 2A_rA_{ob}\cos[(k_r + k_o)y + \phi]$$

$$+ 2A_rA_o\cos[(k_r + k_o)y] + 2A_oA_{ob}\cos\phi\}$$

$$= 2\rho g\{\alpha\cos[(k_r + k_o)y + \phi] + \beta\cos[(k_r + k_o)y] + \gamma\cos\phi + \tfrac{1}{2}\kappa\}$$

$$- 2C_s\{[(\frac{\partial^2\alpha}{\partial x^2} + \frac{\partial^2\alpha}{\partial y^2}) - \alpha[(\frac{\partial\phi}{\partial x})^2$$

$$+ (\frac{\partial\phi}{\partial y} + k_r + k_o)^2]]\cos[(k_r + k_o)y + \phi] + [(\frac{\partial^2\beta}{\partial x^2} + \frac{\partial^2\beta}{\partial y^2})$$

$$- \beta(k_r + k_o)^2]\cos[(k_r + k_o)y] + [(\frac{\partial^2\gamma}{\partial x^2} + \frac{\partial^2\gamma}{\partial y^2}) - \gamma[(\frac{\partial\phi}{\partial x})^2$$

$$+ (\frac{\partial\phi}{\partial y})^2]]\cos\phi - [2([\frac{\partial\alpha}{\partial x}\frac{\partial\phi}{\partial x} + \frac{\partial\alpha}{\partial y}\frac{\partial\phi}{\partial y} + \frac{\partial\alpha}{\partial y}(k_r + k_o)]$$

$$+ \alpha[(\frac{\partial^2\phi}{\partial x^2}) + \frac{\partial^2\phi}{\partial y^2}])\sin[(k_r + k_o)y + \phi]$$

$$- 4\frac{\partial\beta}{\partial y}(k_r + k_o)\sin[(k_r + k_o)y] \qquad (8)$$

$$- 2[2(\frac{\partial\gamma}{\partial x}\frac{\partial\phi}{\partial x} + \frac{\partial\gamma}{\partial y}\frac{\partial\phi}{\partial y}) + \gamma(\frac{\partial^2\phi}{\partial x^2} + \frac{\partial^2\phi}{\partial y^2})]\sin\phi + \frac{\partial^2\kappa}{\partial y^2}\}$$

Equation (8) is very complicated. However, if it is assumed that the following conditions are satisfied;

$$(k_r + k_o) >> \frac{\partial\phi}{\partial y}, \frac{\partial\phi}{\partial x}$$

$$\alpha(k_r + k_o)^2 >> \frac{\partial^2\alpha}{\partial x^2} + \frac{\partial^2\alpha}{\partial y^2}$$

$$\beta(k_r + k_o)^2 >> \frac{\partial^2\beta}{\partial x^2} + \frac{\partial^2\beta}{\partial y^2}$$

$$\frac{\partial\alpha}{\partial x} \simeq 0$$

$$\frac{\partial\alpha}{\partial y} \simeq 0$$

$$\frac{\partial\beta}{\partial y} \simeq 0 \qquad (9)$$

$$\frac{\partial\gamma}{\partial x} \simeq 0$$

$$\frac{\partial\gamma}{\partial y} \simeq 0$$

$$\frac{\partial^2\phi}{\partial x^2} + \frac{\partial^2\phi}{\partial y^2} \simeq 0$$

$$\rho g\kappa >> c_s\left(\frac{\partial^2\kappa}{\partial x^2} + \frac{\partial^2\kappa}{\partial y^2}\right)$$

then the right-hand side of Equation (8) can be greatly simplified and becomes

$$\begin{aligned}
&\frac{1}{\rho v_s^2}\{A_r^2 + A_{ob}^2 + A_o^2 + 2A_r A_{ob}\cos[(k_r + k_o)y + \phi] \\
&\quad + 2A_r A_o \cos[(k_r + k_o)y] + 2A_o A_{ob}\cos\phi\} \\
&= 2\alpha\,[\rho g + c_s(k_r + k_o)^2]\cos[(k_r + k_o)y + \phi] \qquad (10) \\
&\quad + 2\beta[\rho g + C_s(k_r + k_o)^2]\cos[(k_r + k_o)y] \\
&\quad + 2\gamma\,\rho g\cos\phi + \rho g\kappa \quad .
\end{aligned}$$

From the above Equation, one finds

$$\alpha = \frac{A_r A_{ob}}{\rho v_s^2 [\rho g + c_s (k_r + k_o)^2]} \quad , \tag{11}$$

$$\beta = \frac{A_r A_o}{\rho v_s^2 [\rho g + c_s (k_r + k_o)^2]} \quad , \tag{12}$$

$$\gamma = A_o A_{ob} / (\rho^2 g v_s^2) \quad , \tag{13}$$

$$\kappa = [A_r^2 + A_{ob}^2 + A_o^2] / (\rho^2 g v_s^2) \quad . \tag{14}$$

The solution in the form of Equation (B1) is rewritten as follows:

$$z_s = 2\alpha \cos[(k_r + k_o)y + \phi] + 2\beta \cos[(k_r + k_o)y] + 2\gamma \cos \phi + \kappa \tag{15}$$

The physical meaning of Equation (15) is described below. There is a bulge of height $2\gamma \cos \phi(x,y) + \kappa$ in the area over which the acoustical wave is applied. Impressed upon this bulge are two interference patterns of the same spatial wave number, $k_r + k_o$, but different amplitudes $2\alpha$ and $2\beta$. One of the pattern is different from the other by a phase $\phi(x,y)$. If the reference beam Number 1 is set to zero, i.e., $A_r = 0$, then from Equations (11) and (12) $\alpha = \beta = 0$ and $\kappa = (A_{ob}^2 + A_o^2)/(\rho^2 g v_s^2)$. The bulge is slightly reduced in height, and the interference patterns still exist. The object geometry still modifies the liquefied surface, similar to the case of an in-line hologram. On the other hand, if the reference beam Number 2 is zero, i.e., $A_o = 0$, Equation (15) becomes

$$z_s = 2\alpha \cos[(k_r + k_o)y + \phi] + \kappa' \quad , \tag{16}$$

where

$$\kappa' = (A_r^2 + A_{ob}^2)/(\rho^2 g v_s^2) \quad . \tag{17}$$

Equation (16) represents the interference patterns resulting from a typical off-axis hologram.

## B. Optical Reconstruction of the Acoustical Surface Hologram

The detection of the acoustical hologram can be achieved by the technique of coherent optical image reconstruction. Assume that a laser beam plan wave of amplitude $A_\ell$ and wavelength $\Lambda$ is normally incident (oblique incidence is also possible with more complication in mathematical manipulation) on the surface where the acoustical hologram is recorded. The light beam is expressed by

$$s(z) = A_\ell e^{-j\frac{2\pi}{\Lambda} z} = A_\ell e^{-jk_\ell z} \tag{18}$$

where $k_\ell = \frac{2\pi}{\Lambda}$ is the wave number of the light wave.

After reflection from the surface hologram, the amplitude s(z) is reduced to R and the phase of the beam is modified by 2 $z_s(x,y)$ where $z_s(x,y)$ is in general given by Equation (15). The reflected light beam may then be written as

$$\begin{aligned} S_r(x,y) = R\, e^{jk_\ell z}\, e^{j2k_\ell z_s} \\ + R\, e^{-jk_\ell z} \exp[2jk_\ell\{2\alpha \cos[(k_r + k_o)y + \phi] \\ + 2\beta \cos[(k_r + k_o)y] \\ + 2\gamma \cos \phi + \kappa\}] \quad . \end{aligned} \tag{19}$$

Since

$$\exp[j\, a \cos b] = \sum_{n=-\infty}^{\infty} j^n J_n(a) \exp(-jnb) \quad , \tag{20}$$

where $J_n$ is the $n^{th}$ order Bessel function, Equation (19) can be expressed in terms of the Bessel functions as

$$S_r(x,y) = R\, e^{jk_\ell(z + 2\kappa)}$$

$$\cdot\{\sum_{n=-\infty}^{\infty} j^n J_n(4\alpha k_\ell) e^{-j[n(k_r + k_o)y + n\phi]}\}$$

$$\cdot\{\sum_{n=-\infty}^{\infty} j^n J_n(4\beta k_\ell) e^{-j[n(k_r + k_o)y]}\}$$

$$\cdot\{\sum_{n=-\infty}^{\infty} j^n J_n(4\gamma k_\ell) e^{-jn\phi}\} \qquad (21)$$

The property of $J_n(x)$ indicates that when a is sufficiently small, $J_o(a)$ approaches 1, $J_{-1}(a)$ approaches $\frac{a}{2}$, $J_{-1}(a)$ approaches $-\frac{a}{2}$, and $J_n(a)$ for n not equal to -1, 0, or 1 approaches 0. Therefore if $4\alpha k_\ell$, $4\beta k_\ell$, and $4\gamma k_\ell$ are all sufficiently small, $S_r(x,y)$ can be approximately given by

$$S_r(x,y) = R\, e^{jk_\ell(z + 2\kappa)}$$

$$\cdot\{1 + j^{2\alpha k_\ell} e^{-j[(k_r + k_o)y + \phi]} + j2\alpha k_\ell e^{j[(k_r + k_o)y + \phi]}\}$$

$$\cdot\{1 + j2\beta k_\ell e^{-j[(k_r + k_o)y + \phi]} + j2\beta k_\ell e^{j[(k_r + k_o)y + \phi]}\}$$

$$\cdot\{1 + j2\gamma k_\ell e^{-j\phi} + j2\gamma k_\ell e^{-j\phi}\} \; . \qquad (22)$$

Expansion of Equation (22) yields

$$S_r(x,y) = R\, e^{jk_\ell(z + 2\kappa)}$$

$$\{1 + j\,2[(\alpha k_\ell + \beta k_\ell)e^{-j(k_r + k_o)y} + \gamma k_\ell]e^{-j\phi}$$

$$+ j\,2[(\alpha k_\ell + \beta k_\ell)e^{j(k_r + k_o)y} + \gamma k_\ell]e^{j\phi}$$

$$- \text{[}16\,\gamma\beta k_\ell^2 \cos\phi \cos[(k_r + k_o)y + \phi]$$

$$+ 16\,\alpha\beta k_\ell^2 \cos^2[(k_r + k_o)y + \phi]$$

$$+ 16\,\alpha\gamma k_\ell^2 \cos\phi \cos[(k_r + k_o)y + \phi]\ \text{]}\ \}$$

$$\simeq R\, e^{jk_\ell(z + 2\kappa)}\{1 + j\,2[(\alpha k_\ell + \beta k_\ell)e^{-j(k_r + k_o)y} + \gamma k_\ell]e^{-j\phi}$$

$$+ j\,2[(\alpha k_\ell + \beta k_\ell)e^{j(k_r + k_o)y} + \gamma k_\ell]e^{j\phi}\} \qquad (23)$$

The reason that the terms in [ ] in the above equation can be omitted is not only because they are negligibly small in comparison to 1 but also that their phases are of no importance to the reconstruction process. What is of importance to the optical image reconstruction is the positive first order diffraction term or the term that contains $e^{-j\phi}$. The phase term is identical to that of the object beam given by Equation (2), and the amplitude $A_{ob}$ of the original object beam is also contained in $\alpha$ and $\gamma$. The following two special cases are considered:

(1) $A_o = 0$ , so that $\beta = 0$ , $\gamma = 0$ ,

$$S'_{r_1}(x,y) = j2\,R\, e^{jk_\ell(z + 2\kappa)}[\alpha k_\ell\, e^{-j(k_r + k_o)y}]e^{-j\phi}$$

$$= S_{r_1}(x,y) \quad . \qquad (24)$$

A spatial filter can be placed in the Fourier plane and the term $S_{r_1}(x,y)$ can be isolated for the holographic image reconstruction.

(2) $A_r = 0$ but $A_o \neq 0$, this implies $\alpha = 0$ and $\beta = 0$, hence

$$S_r(x,y) = j2R\gamma k_\ell \, e^{jk_\ell(z + 2\kappa)} \, e^{-j\phi} \quad . \tag{25}$$

The amplitude and phase of the object beam is still contained in $S_r(x,y)$.

Therefore the image of the in-line acoustical hologram can also be optically reconstructed by the proper spatial filtering process.

## III. EXPERIMENT

The experiment will be described in four parts, i.e., device fabrication, heating techniques, the acoustical holographic system, and the experimental results.

### A. Device Fabrication

The thermoplastic device that has been investigated has three different configurations according to the different heating techniques applied to the device. These device structures are illustrated in *Figures 2* through *4*. Basically the device consists of a uniform and extremely flat layer of thermoplastic material coated on a flat substrate.

*Figure 2* shows a device with a glass substrate. The glass with a thin coating of (indium oxygen) InO is supplied by Pittsburgh Plate Glass Company. The InO layer serves as a resistive heating element and hence is connected by the metal electrodes (either copper or aluminum) to an electric power supply. A thin thermoplastic layer is coated on InO. The figures are not drawn to proportion because in reality the substrate is several orders of magnitude thicker than the thermoplastic layer.

*Figure 3* shows a device structure that basically consists of a layer of thermoplastic material coated on the upper external surface of a pillbox type substrate. The internal space of the pillbox can be supplied with temperature-controlled water. Through the control of the temperature and the flow-rate of the water, the thermoplastic temperature can be adjusted.

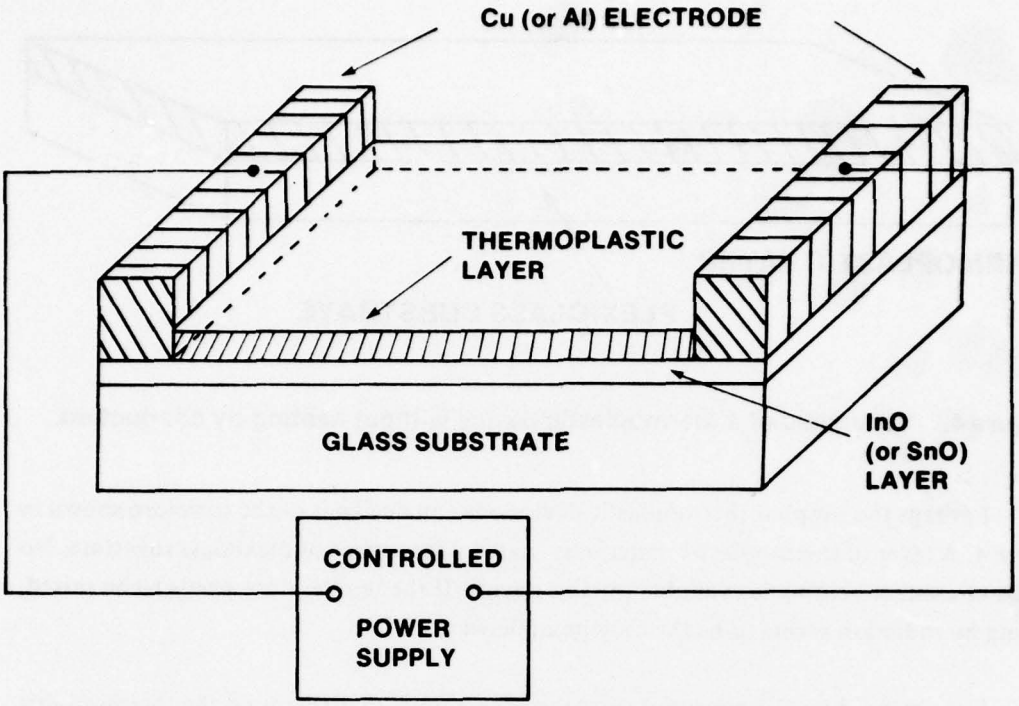


**Figure 2. Schematic of a thermoplastic device with electric heating.**

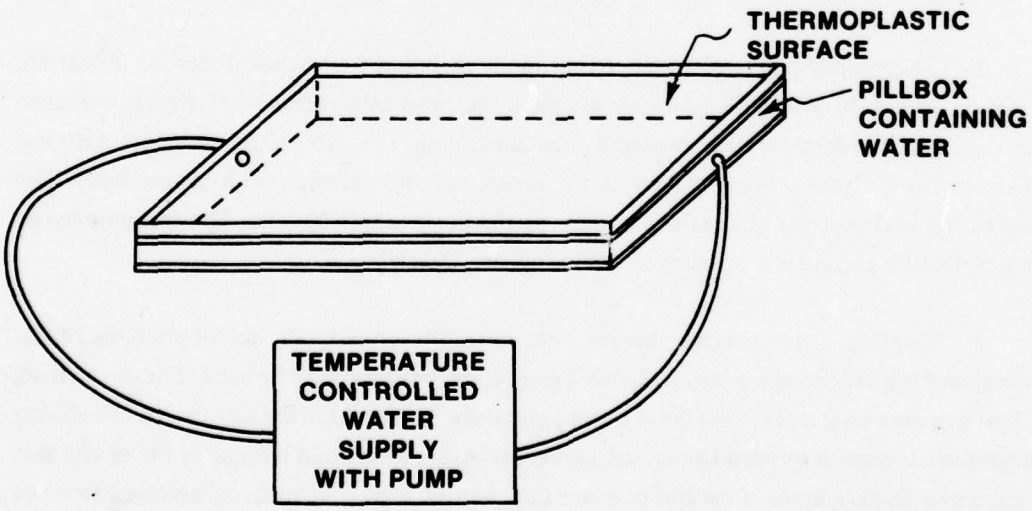


**Figure 3. Schematic of a thermoplastic device with hot water heating.**

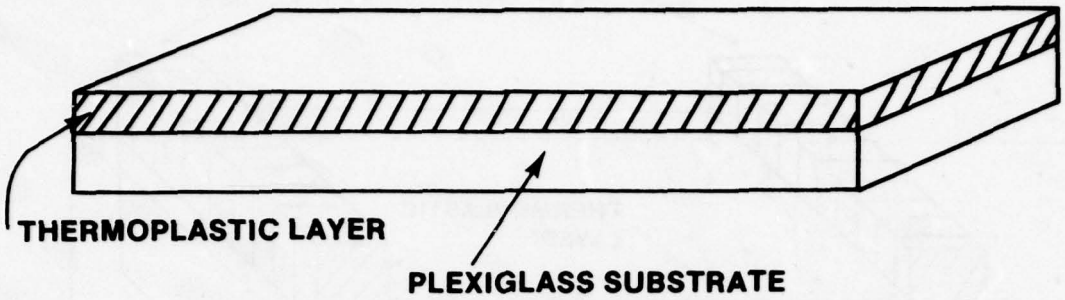


**Figure 4. Schematic of a thermoplastic device without heating by conduction.**

Perhaps the simplest thermoplastic device one can design is of the structure shown in *Figure 4*. A layer of thermoplastic material is coated over a piece of plexiglass substrate. No means of contact heating is available for this device. If the temperature needs to be raised, heating by radiation seems to be the only possible way.

Not sketched in *Figures 3* and *4* are the edge guards that surround the thermoplastic layer. The reason for their existence will be clear after the coating techniques are described.

Additional specific descriptions of the device are given as follows:

1. Thermoplastics used in the experiment included Staybelite, Ester 10, Foral 85, S-25, S-55, and S-70. All these materials are pale, thermoplastic resins with strong resistance to oxidation and to discoloration caused by heat and aging. They are soluble in esters; ketones; higher alcohols; glycol ethers; and aliphatic, aromatic, and chlorinated hydrocarbons. The solvent used in dissolving the resins for making the devices was hexane. The thermoplastics was supplied by Hercules Company of Wilmington, Delaware.

2. Coating of the thermoplastics were normally done in the past by means of dip coating, and high speed spinning. A Fisher dip coating machine may be used. The dip coating method can only coat a very thin layer (approximately 1$\mu$). Though the layer is quite uniform and smooth, it cannot be used for acoustical recording as was found later after the device was tested. For a thicker layer, a special new method was devised. The method involved first the measurement of an exact amount of the thermoplastic resin, making a solution of the measured thermoplastic, and spreading the resin uniformly over the flat substrate (of the device) guarded by the edge guard. The evaporation of the solvent leaves a uniform layer of

thermoplastic on the substrate. The thickness of the layer can be easily calculated. During the evaporation process, it is important that the substrate be placed in both a level and stable position.

3. The etching and masking process follows standard microelectronic laboratory procedures. The etching of InO can be done by diluting 37% HCl to a 19% solution and leaving the InO in the diluted 65° C solution for 4 to 5 minutes. Exact temperature control is important if repeatable results are needed. If 3% Nitrite is added, the etching time can be reduced to one minute or so.*

## B. Heating Techniques

To record acoustical wave patterns, it is necessary first to soften the thermoplastic layer by heating. Various heating methods are described below.

1. Electric heating by a resistive element can be performed by the circuit as sketched in *Figure 5*. The two transistors (2N3773) are triggered by an electric pulse of various pulse periods. Single pulse, double pulse or a sequence of pulses can be made available by selecting a

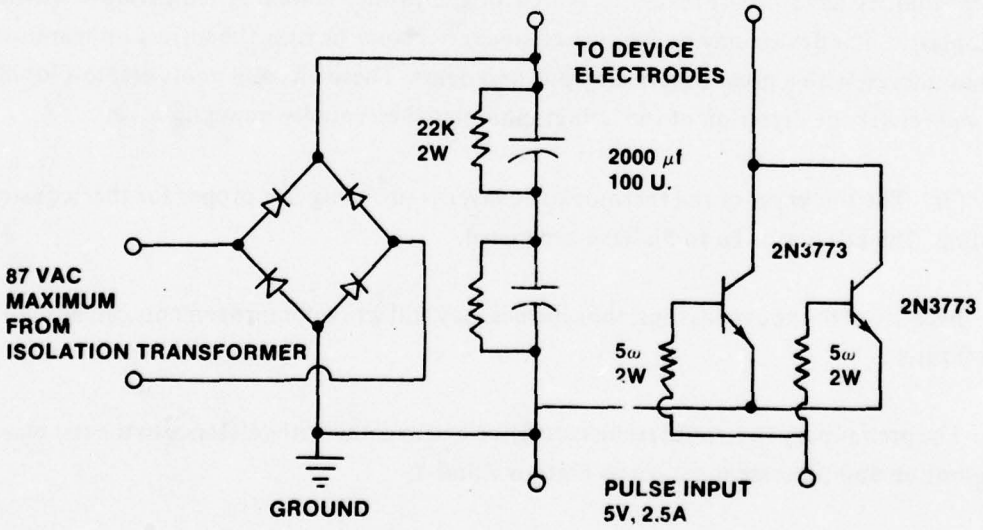


**Figure 5. Electric pulse-controlled dc. power supply circuit.**

*The method is suggested by Optical Coating Laboratories, Inc. according to N.C. Stewart and L.S Cosentino of RCA. (609/452-2700).

proper pulse generator. D.C. voltage up to 110 volts can be applied to the heating element of the thermoplastic device.

Hot water heating can be performed by pumping temperature controlled water through the pillbox as shown in *Figure 3*. The control of the temperature can be achieved by using a temperature regulator. The circuit diagram and operation of the temperature regulator is given in Appendix C.

## C. Experimental Results

Many attempts were tried to record a hologram on the thermoplastic surface. All three device structures as shown in *Figures 2* through *4* have been fabricated and tested in the acoustical holographic system as illustrated** in detail in *Figure 6*.[25] In the following, first the failures and then the successes of the experiment are reported.

The electric heating and hot water heating schemes have not been successful. This is probably mainly due to the following reasons:

(1) The thermoplastic layers are placed in contact with the water surface. Trial and error techniques have been applied in search of the proper softening temperature of the thermoplastic. The device may be overheated since after some heating the surface appearance becomes uneven with a great deal of tiny pits and dents. These pits and dents create a lot of noise and render the detection of the holographic signal essentially impossible.

(2) The thickness of the thermoplastic layer is probably not proper for the acoustic recording. Thicknesses of $1\mu$ to $5\mu$ have been tried.

Because of the above reasons, the schemes may still work if improvements can be made in the future.

The preliminary successful results are described in detail with reference to the test plate configuration and placement shown in *Figures 7* and *8*.

---

**Courtesy of Reference 25.

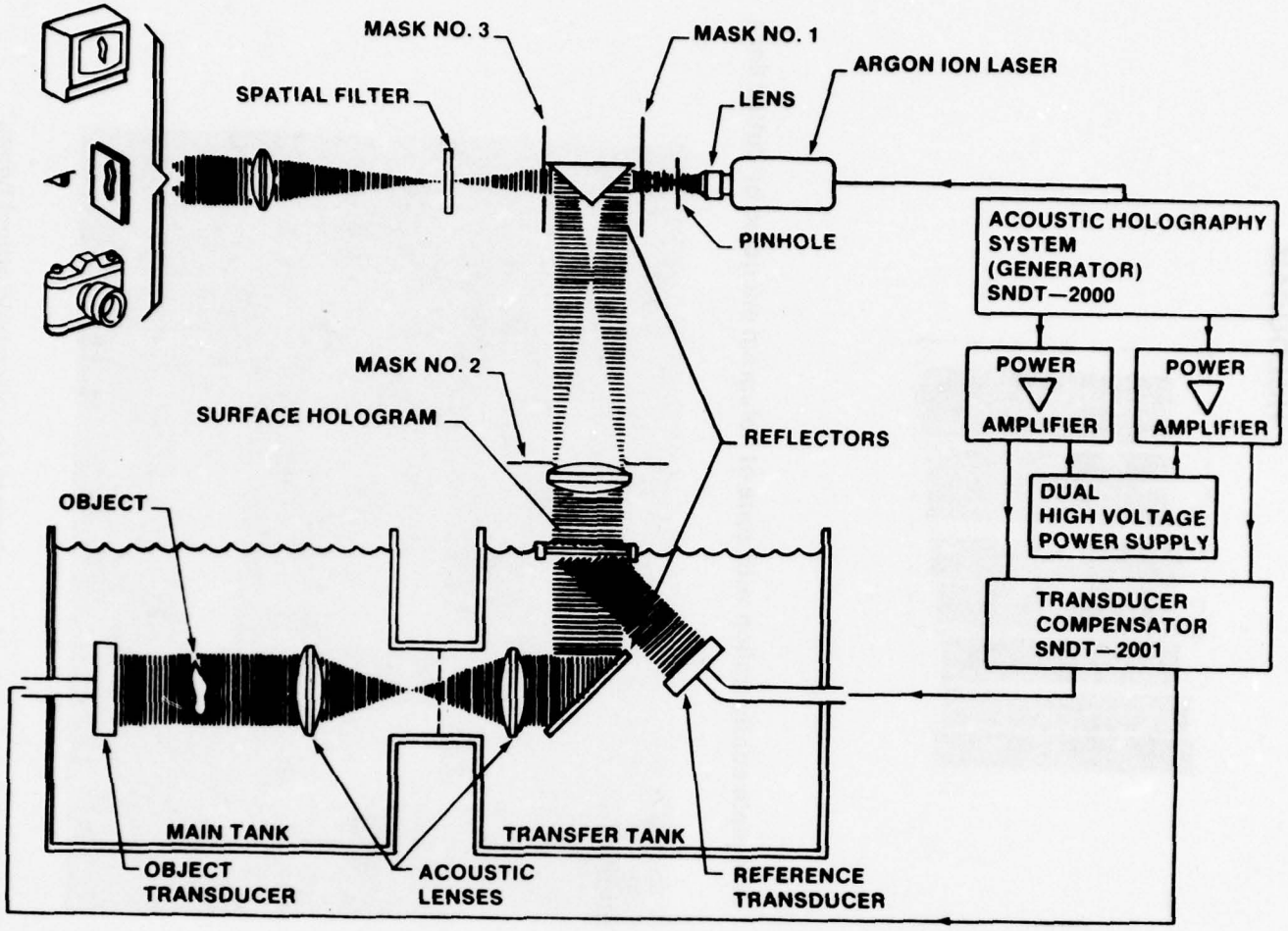


**Figure 6. Acoustical holographic and coherent optical image detection system.**

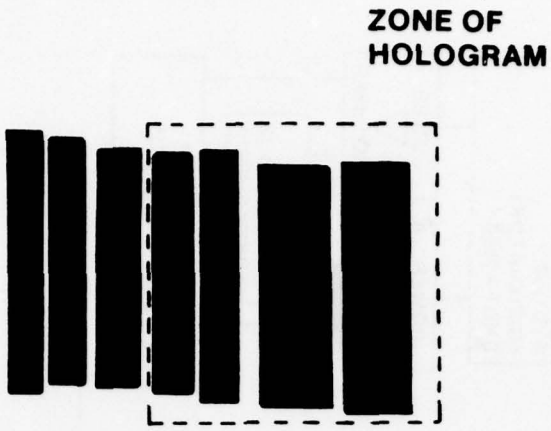


**Figure 7. Test plate configuration with zone of hologram encircled by dotted lines.**

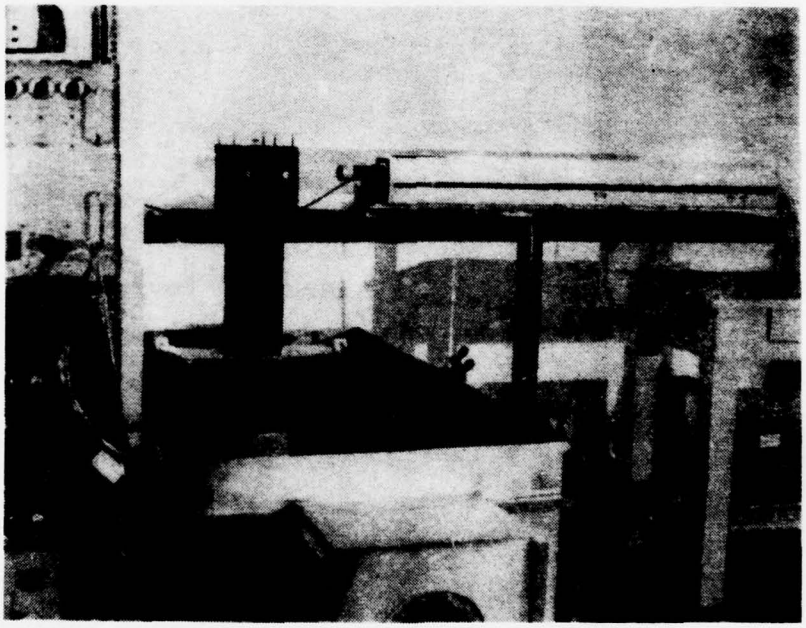

**Figure 8. A test plate at a position in the ultrasonic object beam.***

*Courtesy of Reference 25.

Several devices made according to the structure shown in *Figure 4* were tested. Since there was no direct heating mechanism being built in the device, what was chosen was a thermoplastic (S-25) of especially low softening temperature of 25° C. The material was sticky and could be made to flow slowly at room temperature. A thickness of around 1250$\mu$ of S-25 was coated on the plexiglass substrate. A photograph of one of the devices is shown in *Figure 9*. The area of the recording surface was approximately 17 × 20 cm. This is larger than any other thermoplastic recording devices previously experimented and reported on in the literature. (Optical thermoplastic devices are usually of a dimension of 1 × 1 cm.) The lighted region in the center of the device is from a 2-W argon laser source used for optical image reconstruction.

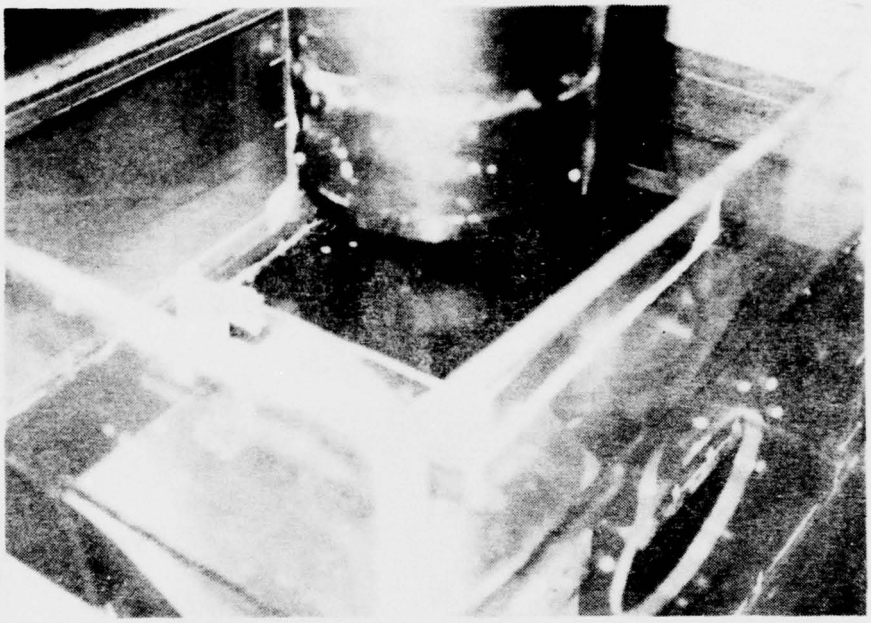

**Figure 9. A thermoplastic device under the six-inch diameter lens cylinder. The device, sitting on water, is in the recording and reconstruction conditions.**

The device was placed in the acoustical holographic system with its thermoplastic surface facing up to the air. After its surface settled to a completely level position (since the thermoplastic surface has changed shape during the moving and positioning process), the optical reconstruction was recorded by a polaroid film at the image plane and is shown in *Figure 10(a)*. After the acoustical beams of 3 MHz from both the reference and the object beam acoustical transducers were applied a few seconds later, the reconstructed image of the surface was again recorded and shown in *Figure 10(b)*. The image was retained for over 2

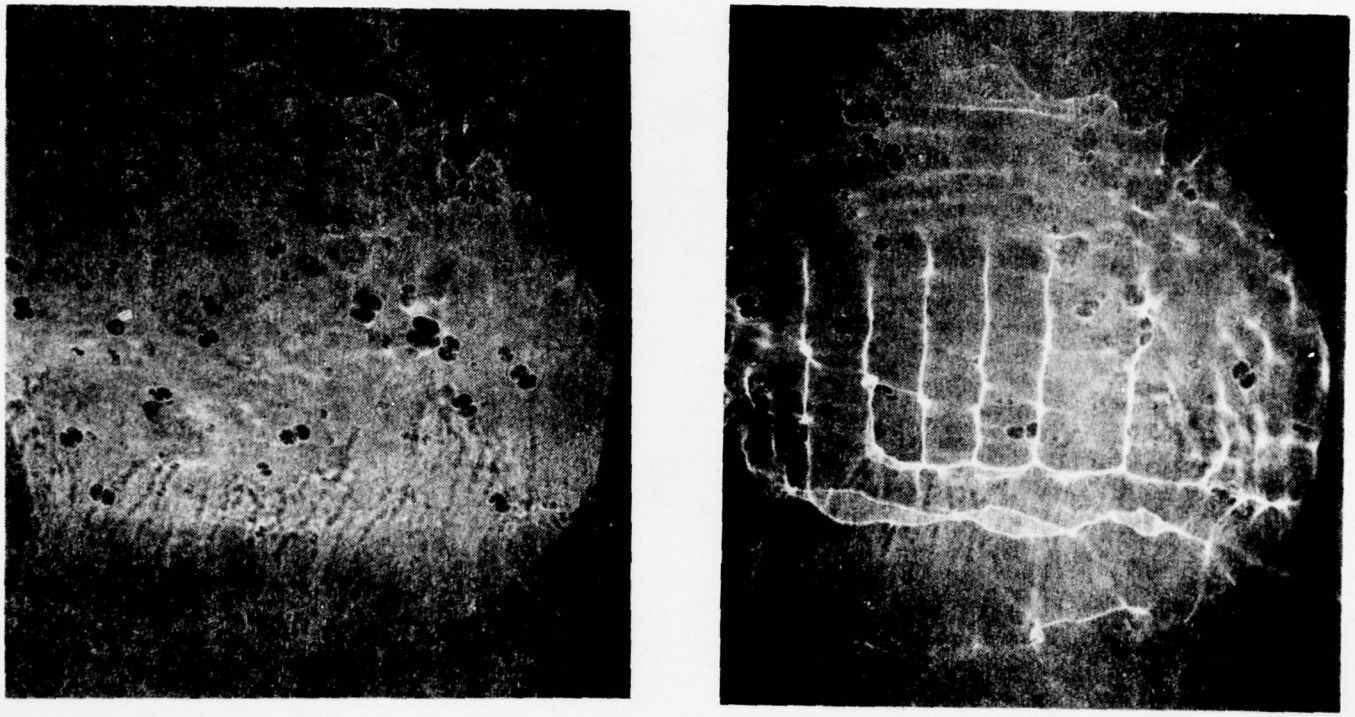

(a) (b)

Figure 10. Coherent optical image reconstruction of the thermoplastic surface (a) without a hologram, (b) with a hologram. The real size of the recording area is about 7 × 7 cm.

minutes after the acoustical beams were turned off. The gradual disappearance of the imag probably due to gravitation and surface tension because the thermoplastic was in a softened form even at room temperature. A great deal of hexane was still inside the resin. Repeated writing and erasure at room temperature has shown similar phenomena. Another interesting phenomenon observed was that when the reference beam alone was applied, no image of the object appeared but if the object beam was applied by itself, the outline of the object in the image was very similar to that shown in *Figure 10(b)*. This indicated that, according to the theoretical analysis, due to the structural simplicity of the object; an in-line hologram was recorded.

Another device of 20 × 28.6 cm was fabricated with a 1.25 mm S-25 thermoplastic layer. The top surface of the substrate that was in contact with the thermoplastic was painted black so that reflections could be reduced. The device was allowed to stand for about one month so that most of the hexane was evaporated from the thermoplastic. It was then replaced in the system and tested. *Figure 11(a)* is a photograph showing the real-time *in situ* coherent optical image reconstruction of the thermoplastic surface without the recording of any acoustical hologram; where *Figure 11(b)*, is the same surface with an acoustical hologram and with all acoustical beams off. It shows that the dotted line enclosed portion of the test-plate as shown in *Figure 7* can be vaguely discerned in the noise. The noise arises due to the dust particles as shown in *Figure 11(a)* and due to the influence of the hexane that still could be trapped inside the thermoplastic. Both problems can be solved with further work. Optical spatial filtering would not solve these problems so that no filtering process was included while these photographs were taken.

One feature of this hologram device is that it can retain the image at room temperature for over 30 minutes, much longer than the corresponding image of *Figure 10(b)*. For purpose of comparison, a water surface hologram was taken next and shown in *Figure 11(c)*. The hologram was recorded with the object in the same position and the system configuration was also the same; only the ratio between reference and object beam intensities was changed. It can be seen that the water surface was not much better in resolution although in both cases optimization was not attempted. Naturally the water surface hologram faded away almost immediately when the acoustic beams were turned off; this feature is distinctively different from that of the thermoplastic holograms.

## IV. DISCUSSION

The acoustical hologram recorded by the thermoplastic device as shown in *Figure 10* is far from perfect. The image has a great deal of noise even without any acoustical signal. This is

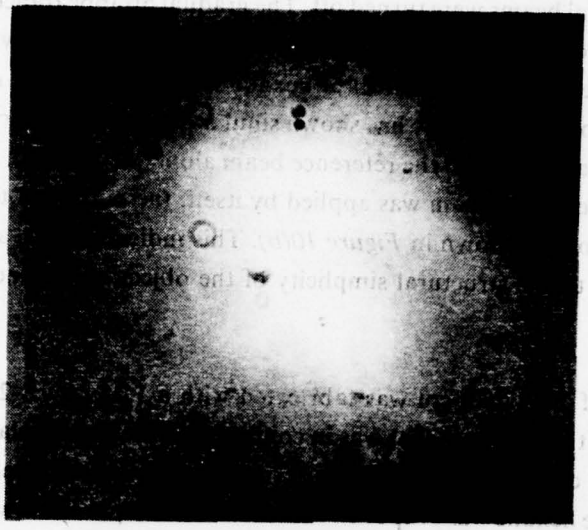

(a)

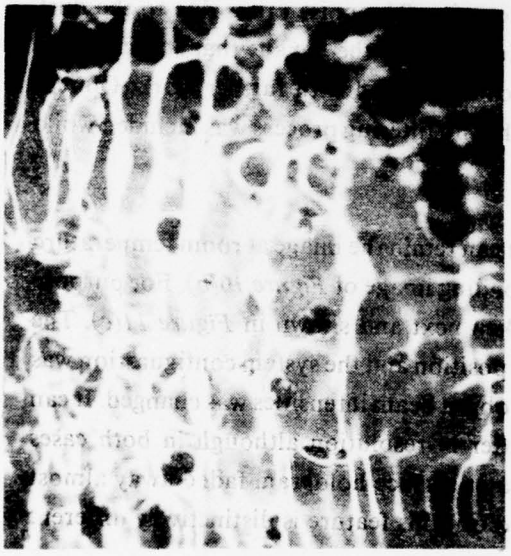

(b)

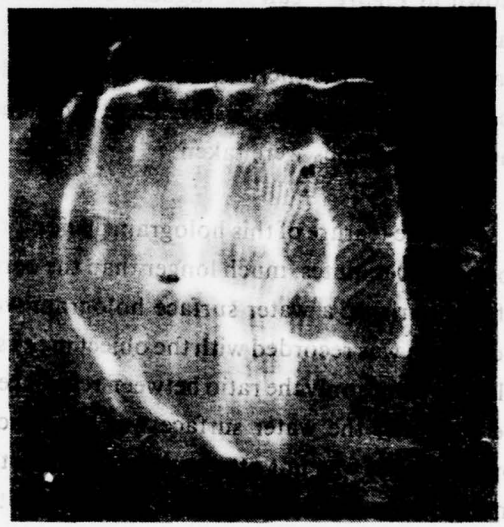

(c)

**Figure 11. Photograph of real-time *in situ* coherent optical image reconstruction of (a) thermoplastic surface without recording an acoustical hologram; (b) thermoplastic hologram with acoustical beams turned off; and (c) water surface hologram with acoustical beams on. No optical spatial filtering process was included.**

because the surface of the thermoplastic layer was not made perfect. Additional possible reasons are described as follows. Acoustical powers and the power ratio between reference and object beams is not optimized; the holographic system configuration is not optimized (it should be improved). The thickness of the thermoplastic layer for the recording of the 3 MHz signal was not optimized. No temperature control unit is included because no heat is applied. No spatial filtering was performed. All this can be remedied with added effort.

Nevertheless, the preliminary result obtained is encouraging because:

- It is the first time that an *in situ* real-time recording and simultaneous optical reconstruction of an acoustical hologram on a thermoplastic device has been achieved.

- The recording area is larger than any other thermoplastic device reported to date.

- The image demonstrates that the softened thermoplastic can be used for the recording of acoustical holograms.

- The capability of retention of the holographic image demonstrates the memory function of the thermoplastic material with respect to the interference patterns of the acoustical waves. In contrast, water surface holograms have no retention capability.

- The capability of repeated erasures and recordings of the device has shown its re-usability.

- No dark handling was needed.

Judging from the result so far, it is concluded that additional, continued investigations, both theoretical and experimental, are justified. The topics should include but not be limited to the following areas:

- Various uniform heating and accurate temperature control systems for the device.

- Speed and repeatability control and improvement.

- Various thermoplastics for the device.

- Thickness variations versus acoustical frequency.

- Optical filtering techniques for improving the signal-to-noise ratio of the reconstructed image.

- Optimization of the substrate being used for device construction.

- Consideration of using reflective thermoplastic for improving the detection of the signals.

- Double exposure acoustical holographic recording by thermoplastic devices.

- Recording of reflective acoustical holograms.

- Applications of the device for acoustical speckle hologram nondestructive testing (HNDT).

- Large system integration.

- Other applications of thermoplastic recordings such as acoustical image processing.

The results of the theoretical and experimental investigations shown in this report leads one to believe that after further intensive studies of the thermoplastic device as recommended in the above, this device should become a very promising new device for *in situ* real-time recording and read-out of acoustical holographic images. It has great potential in nondestructive testing and other engineering and biomedical applications.

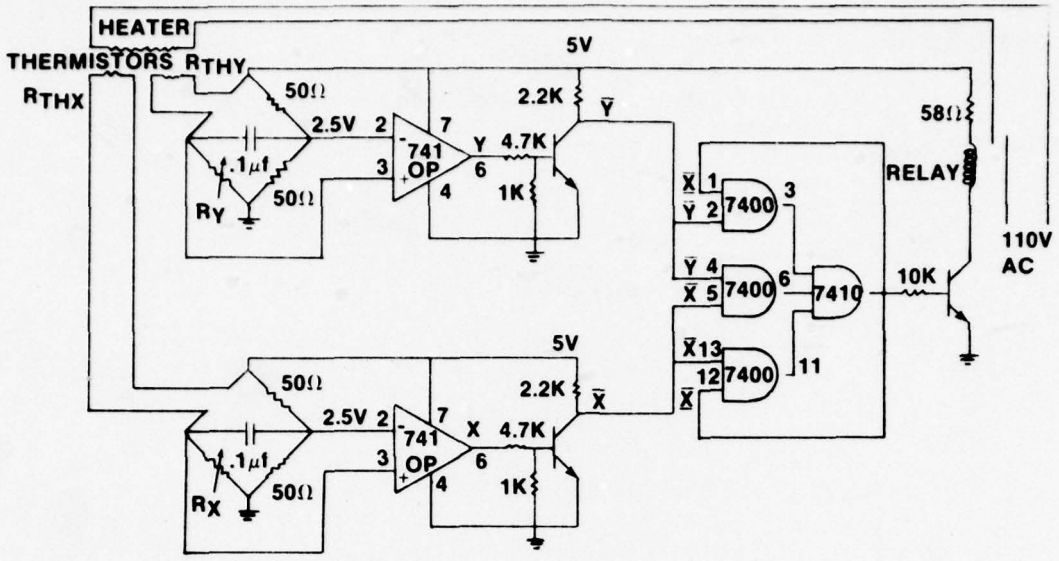


Figure C-1. Circuit diagram.

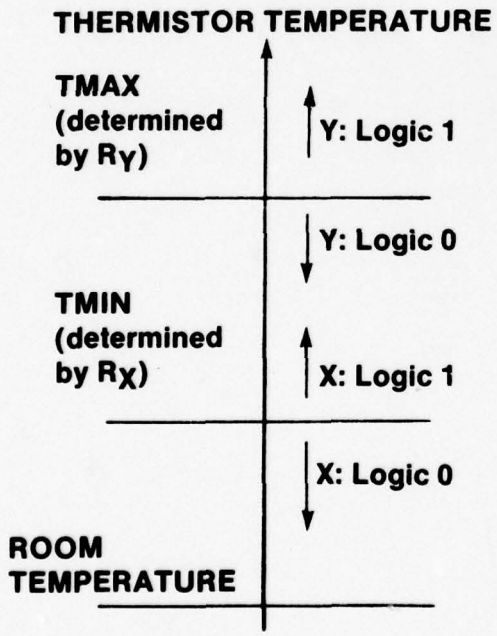


Figure C-2. Logic definition.

$Z^+$: Logic 1 (heater on)
Logic 0 (heater off)

| X | Y | Z | $Z^+$ |
|---|---|---|---|
| 0 | 0 | 0 | 1 |
| 0 | 0 | 1 | 1 |
| 1 | 0 | 1 | 1 |
| 1 | 1 | 1 | 0 |
| 1 | 1 | 0 | 0 |
| 1 | 0 | 0 | 0 |
| 0 | 0 | 0 | 1 |

Figure C-3. Truth table.

Blank

# REFERENCES


1. Glenn, W.E., "Thermoplastic Recording," *Applied Physics*, Volume 30 (1959), p. 1870.

2. Gaynor, J. and Aftergut, S., "Photoplastic Recording," *Photographic Science Engineering*, Volume 7 (1963), p. 209.

3. Wolff, N.E., "A Photoconductive Thermoplastic Recording System," *RCA Review*, Volume 25 (1964), p. 200.

4. Giaimo, E.C., "Thermoplastic Organic Photoconductive Recording Media-Electrophotographic Characteristics and Processing Techniques," *RCA Review*, Volume 25 (1964), p. 692.

5. Urbach, J.C. and Meier, R. W., "Thermoplastic Xerographic Holography," *Applied Optics*, Volume 5 (1966).

6. Lin, L.H. and Beauchamp, M.L., "Write-Read-Erase *in Situ* Optical Memory Using Thermoplastic Holograms," *Applied Optics*, Volume 9 (1970), p. 2088.

7. Credelle, T.L. and Spong, F.W., "Thermoplastic Media for Holographic Recording," *RCA Review*, Volume 33 (1972), p. 206.

8. Colburn, W.S. and Tompkins, E.N., "Improved Thermoplastic Photoconductor Devices for Holographic Recording," *Applied Optics*, Volume 12 (1974), p. 2934.

9. Colburn, W.S. and DuBow, J.B., "Photoplastic Recording Materials," Final Technical Report AFAL-TR-73-255, August 1973.

10. Fienup, J.R., "Optical Processors Using Holographic Optical Elements," Final Technical Report, Report No. 119400-2-F, Environmental Research Institute of Michigan, Ann Arbor, April 1978.

## REFERENCES (Continued)


11. Schaffert, R.M., "A New High-Sensitivity Organic Photoconductor for Electrophotography," *IBM Journal of Research and Development*, Volume 15 (1971), p. 75.

12. Bergen, R.F., "Characterization of a Xerographic Thermoplastic Holographic Recording Material," *Photographic Science and Engineering*, Volume 17 (1973), p. 473.

13. Kriz, K. "Spectral Response and Sensitometric Curves of Doped Poly-N-Vinylcarbazole Films in Electrophotography Under Positive and Negative Charging Modes," *Photographic Science and Engineering*, Volume 16 (1972), p. 58.

14. Anderson, H.R., Jr., Bartkus, E.A., and Reynolds, J.A., "Molecular Engineering in the Development of Materials for Thermoplastic Recording," *IBM Journal of Research and Development*, Volume 15 (1971), p. 140.

15. Urbach, J.C. and Meier, R.W., "Properties and Limitations of Hologram Recording Materials," *Applied Optics*, Volume 8 (1969), p. 2269.

16. Falconer, D.G., "Role of the Photographic Process in Holography," *Photographic Science and Engineering*, Volume 10 (1966), p. 133.

17. Cathey, W.T., *Optical Information Processing and Holography*, Wiley & Sons, New York, pp. 68-70.

18. Maloney, W.T. and Gravel, R.L., "Submillisecond Development of Thermoplastic Recordings," *Aplied Optics*, Volume 13 (1974), p. 2471.

19. Gill, W.D., "Drift Mobilities in Amorphous Charge-Transfer Complexes of Trinitrofluorenone and Poly-n-vinylcarbazole," *Journal of Applied Physics*, Volume 43 (1972), p. 5033.

20. Lo, D.S., Johnson, L.H., and Honebrink, R.W., "Thermoplastic Recording," *SPIE Proceedings on Practical Applications of Low Power Lasers*, Volume 92, San Diego, California, August 26-27, 1976.

## REFERENCES (Concluded)


21. Reich, S., Rav-Noy, Z., and Friesem, A.A., "Frost Suppression in Photoconductor-Thermoplastic Holographic Recording Devices," *Applied Physics Letters*, Volume 31 (1977), p. 654.

22. Saito, T., Oshima, S., Honda, T., and Teujiuchi, J., "An Improved Technique for Holographic Recording on a Thermoplastic Photoconductor," *Optical Communications*, Volume 16 (1976), p. 90.

23. Young, J.D. and Wolfe, J.E., "A New Recording Technique for Acoustic Holography," *Applied Physics Letters*, Volume 11 (1967), p. 294.

24. Brenden, B.B., *Optical and Acoustical Holography*, Editor: E. Cannatini (Plenum Press, N.Y.) (1972).

25. Irelan, V.G., Mullinix, B.R., and Castle, J.G., "Real-time Acoustical Holography Systems," Technical Report T-78-10, US Army Missile Research and Development Command, October 1977.

Blank

# APPENDIX A

Blank

## DEVIATION OF EQUATION (10)

$$\rho(x,y) = \frac{1}{\rho v_s^2} \left| A_r \exp jk_r y + A_{ob} \exp [-j(k_o y + \phi(x,y)] + A_o \exp (-j k_o y) \right|^2$$

$$= \frac{1}{\rho v_s^2} \left| [A_r \cos k_r y + A_{ob} \cos(k_o y + \phi(x,y)) + A_o \cos k_o y] + j [A_r \sin k_r y - A_{ob} \sin[k_o y + \phi(x,y)] - A_o \sin k_o y] \right|^2$$

$$= \frac{1}{\rho v_s^2} \left\{ [A_r \cos k_r y + A_{ob} \cos(k_o y + \phi(x,y) + A_o \cos k_o y]^2 + [A_r \sin k_r y - A_{ob} \sin [k_o y + \phi(x,y)] - A_o \sin k_o y ]^2 \right\}$$

$$= \frac{1}{\rho v_s^2} \left\{ A_r^2 + A_{ob}^2 + A_o^2 + 2 A_r A_{ob} [\cos k_r y \cos[k_o y + \phi(x,y)] - \sin k_r y \sin[k_o y + \phi(x,y)] + 2 A_r A_o [\cos k_r y \cos k_o y - \sin k_r y \sin k_o y] + 2 A_o A_{ob} [\cos k_o y \cos[k_o y + \phi(x,y)] + \sin k_o y \sin[k_o y + \phi(x,y)] \right\}$$

$$= \frac{1}{\rho v_s^2} \left\{ A_r^2 + A_{ob}^2 + A_o^2 + 2 A_r A_{ob} \cos[(k_r + k_o)y + \phi(x,y)] + 2 A_r A_o \cos(k_r + k_o)y + 2 A_o A_{ob} \cos \phi(x,y) \right\} \quad (10)$$

Blank

# APPENDIX B

Blank

Let $\alpha$, $\beta$, $\gamma$, and $\kappa$ be functions of x and y. Assume a steady state solution of Equation (7) be of the form

$$z_s(x,y) = 2\,\alpha \cos[(k_r + k_o)y + \phi(x,y)] + 2\,\beta \cos[(k_r + k_o)y] + 2\,\gamma \cos\phi(x,y) + k\,, \tag{B1}$$

then,

$$\frac{\partial z_s}{\partial x} = 2\,\frac{\partial \alpha}{\partial x} \cos[(k_r + k_o)y + \phi(x,y)] - 2\,\alpha\,\frac{\partial \phi}{\partial x} \sin[(k_r + k_o)y + \phi(x,y)] + 2\,\frac{\partial \beta}{\partial x} \cos[(k_r + k_o)y] + 2\,\frac{\partial \gamma}{\partial x} \cos\phi(x,y) - 2\,\gamma\,\frac{\partial \phi}{\partial x} \sin\phi(x,y) + \frac{\partial k}{\partial x}\,, \tag{B2}$$

$$\frac{\partial^2 z_s}{\partial x^2} = 2\,\frac{\partial^2 \alpha}{\partial x^2} \cos[(k_r + k_o)y + \phi(x,y)] - 4\,\frac{\partial \alpha}{\partial x}\,\frac{\partial \phi}{\partial x} \sin[(k_r + k_o)y + \phi(x,y)] - 2\,\alpha \left(\frac{\partial \phi}{\partial x}\right)^2 \cos[(k_r + k_o)y + \phi(x,y)] - 2\,\alpha\,\frac{\partial^2 \phi}{\partial x^2} \sin[(k_r + k_o)y + \phi(x,y)] + 2\,\frac{\partial^2 \beta}{\partial x^2} \cos[(k_r + k_o)y] + 2\,\frac{\partial^2 \gamma}{\partial x^2} \cos\phi(x,y) - 4\,\frac{\partial \gamma}{\partial x}\,\frac{\partial \phi}{\partial x} \sin\phi(x,y) - 2\,\gamma \left(\frac{\partial \phi}{\partial x}\right)^2 \cos\phi(x,y) - 2\,\gamma\,\frac{\partial^2 \phi}{\partial x^2} \sin\phi(x,y) + \frac{\partial^2 k}{\partial x^2}\,, \tag{B3}$$

$$\frac{\partial z_s}{\partial y} = 2 \frac{\partial \alpha}{\partial y} \cos[(k_r + k_o)y + \phi(x,y)]$$

$$- 2\alpha \left[ \frac{\partial \phi}{\partial y} + (k_r + k_o) \right] \sin[(k_r + k_o)y + \phi(x,y)]$$

$$+ 2 \frac{\partial \beta}{\partial y} \cos[(k_r + k_o)y]$$

$$- 2 \beta (k_r + k_o) \sin[(k_r + k_o)y]$$

$$+ 2 \frac{\partial \gamma}{\partial y} \cos \phi (x,y)$$

$$- 2 \gamma \frac{\partial \phi}{\partial y} \sin \phi(x,y) + \frac{\partial k}{\partial y} \quad , \tag{B4}$$

and

$$\frac{\partial^2 z_s}{\partial y^2} = 2 \frac{\partial^2 \alpha}{\partial y^2} \cos[(k_r + k_o)y + \phi]$$

$$- 4 \frac{\partial \alpha}{\partial y} \left( \frac{\partial \phi}{\partial y} + k_r + k_o \right) \sin[(k_r + k_o)y + \phi]$$

$$- 2 \alpha \frac{\partial^2 \phi}{\partial y^2} \sin[(k_r + k_o)y + \phi]$$

$$- 2 \alpha \left( \frac{\partial \phi}{\partial y} + k_r + k_o \right)^2 \cos[(k_r + k_o)y + \phi]$$

$$+ 2 \frac{\partial^2 \beta}{\partial y^2} \cos[(k_r + k_o)y] - 4 \frac{\partial \beta}{\partial y} (k_r + k_o) \sin[(k_r + k_o)y]$$

$$- 2 \beta (k_r + k_o)^2 \cos[(k_r + k_o)y]$$

$$+ 2 \frac{\partial^2 \gamma}{\partial y^2} \cos \phi - 4 \frac{\partial \gamma}{\partial y} \frac{\partial \phi}{\partial y} \sin \phi$$

$$- 2 \gamma \frac{\partial^2 \phi}{\partial y^2} \sin \phi - 2 \gamma \left( \frac{\partial \phi}{\partial y} \right)^2 \cos \phi + \frac{\partial^2 k}{\partial y^2} \quad . \tag{B5}$$

# APPENDIX C

Blank

# I. TEMPERATURE REGULATOR OPERATION PROCEDURE

A. Attach thermistors to heating system.

B. Set "TMAX" and "TMIN" to desired temperature.
(TMAX > TMIN > ROOM TEMP)

C. Turn power switch on.

# II. CIRCUIT DESCRIPTION

There are two identical circuits in *Figure C-1. The top one controls* "TMAX" by changing $R_Y$. The bottom one controls "TMIN" by changing $R_X$. One can preset $R_Y$ ($R_X$) equal to the resistance of thermistor $R_{THY}$ ($R_{THX}$) at the desired temperature "TMAX" ("TMIN"). When the thermistor temperature is higher than "TMAX" ("TMIN"), the output of the OP AMP 741 "Y" ("X") will be a high voltage which is defined as "Logic I". Otherwise the output is low voltage which is defined as "Logic O". The logic definition is shown in *Figure C-2.*

*Figure C-3* shows the states of the logic circuit. The first state "000" means thermistor temperature is lower than "TMIN" and "TMAX" and heater is "OFF". At this time the heater should be turned ON, so $Z^+ = 1$. State "101" means thermistor temperature is higher than "TMIN" but still lower than "TMAX", so the heater should be kept on. State "111" turns the heater off and lets the system cool down to "TMIN", then turns the heater on again.

Blank

# DISTRIBUTION

| | No. of Copies |
|---|---|
| ADTC (DLDSL)<br>Eglin Air Force Base, Florida 32542 | 1 |
| University of California<br>Los Alamos Scientific Laboratory<br>ATTN: Reports Library<br>P.O. Box 1663<br>Los Alamos, New Mexico 87545 | 1 |
| Commander<br>US Army Materiel Development and Readiness Command<br>ATTN: DRCRD<br>DRCDL<br>5001 Eisenhower Avenue<br>Alexandria, Virginia 22333 | 1<br>1 |
| Director<br>Defense Advanced Research Projects Agency<br>1400 Wilson Boulevard<br>Arlington, Virginia 22209 | 1 |
| Defense Technical Information Center<br>Cameron Station<br>Alexandria, Virginia 22314 | 12 |
| Defense Metals Information Center<br>Battelle Memorial Institute<br>505 King Avenue<br>Columbus, Ohio 43201 | 1 |
| Commander<br>US Army Foreign Science and Technology Center<br>ATTN: DRXST-SD3<br>220 Seventh Street, N.E.<br>Charlottesville, Virginia 22901 | 1 |

## DISTRIBUTION (Continued)

| | No. of Copies |
|---|---|
| Office of Chief of Research and Development<br>Department of the Army<br>ATTN: DARD-ARS-P<br>Washington, DC 20301 | 1 |
| Commander<br>US Army Electronics Command<br>ATTN: DRSEL-PA-P<br>-CT-DT<br>-PP, Mr. Sulkolove<br>Fort Monmouth, New Jersey 07703 | 1<br>1<br>1 |
| Commander<br>US Army Natick Laboratories<br>Kansas Street<br>ATTN: STSNLT-EQR<br>Natick, Massachusetts 01760 | 1 |
| Commander<br>US Army Mobility Equipment<br>Research and Development Center<br>Fort Belvoir, Virginia 22060 | 1 |
| Director<br>USA Mobility Equipment Research and Development Center<br>Coating and Chemical Laboratory<br>ATTN: STSFB-CL<br>Aberdeen Proving Ground, Maryland 21005 | 1 |
| Commander<br>Edgewood Arsenal<br>ATTN: SAREA-TS-A<br>Aberdeen Proving Ground, Maryland 21010 | 1 |
| Commander<br>Picatinny Arsenal<br>ATTN: SARPA-TS-S, Mr. M. Costello<br>Dover, New Jersey 07801 | 1 |
| Commander<br>Rock Island Arsenal<br>Research and Development<br>ATTN: 9320<br>Rock Island, Illinois 61201 | 1 |

## DISTRIBUTION (Continued)

| | No. of Copies |
|---|---|
| Commander<br>Watervliet Arsenal<br>Watervliet, New York 12189 | 1 |
| Commander<br>US Army Aviation Systems Command<br>ATTN: DRSAV-EE<br>-MT, Mr. Vollmer<br>St. Louis, Missouri 63166 | 1<br>1 |
| Commander<br>US Army Aeronautical Depot<br>Maintenance Center (Mail Stop)<br>Corpus Christi, Texas 78403 | 1 |
| Commander<br>US Army Test and Evaluation Command<br>ATTN: DRSTE-RA<br>Aberdeen Proving Ground, Maryland 21005 | 1 |
| Commander<br>ATTN: STEAP-MT<br>Aberdeen Proving Ground, Maryland 21005 | 1 |
| Chief<br>Bureau of Naval Weapons<br>Department of the Navy<br>Washington, DC 20390 | 1 |
| Chief<br>Bureau of Ships<br>Department of the Navy<br>Washington, DC 20315 | 1 |
| Naval Research Laboratory<br>ATTN: Dr. M.M. Krafft<br>Code 8430<br>Washington, DC 20375 | 1 |
| Commander<br>Wright Air Development Division<br>ATTN: ASRC<br>Wright-Patterson Air Force Base, Ohio 45433 | 1 |

## DISTRIBUTION (Continued)

| | No. of Copies |
|---|---|
| Director<br>Air Force Materiel Laboratory<br>ATTN: AFML-DO-Library<br>Wright-Patterson Air Force Base, Ohio 45433 | 1 |
| Director<br>Army Materials and Mechanics Research Center<br>ATTN: DRXMR-PL<br>-MT, Mr. Farrow<br>Watertown, Massachusetts 02172 | 1<br>1 |
| Commander<br>White Sands Missile Range<br>ATTN: STEWS-AD-L<br>White Sands Missile Range, New Mexico 88002 | 1 |
| Deputy Commander<br>US Army Nuclear Agency<br>ATTN: MONA-ZB<br>Fort Bliss, Texas 79916 | 1 |
| Jet Propulsion Laboratory<br>California Institute of Technology<br>ATTN: Library/Acquisitions 111-113<br>4800 Oak Grove Drive<br>Pasadena, California 91103 | 1 |
| Sandia Laboratories<br>ATTN: Library<br>P.O. Box 969<br>Livermore, California 94550 | 1 |
| Commander<br>US Army Air Defense School<br>ATTN: ATSA-CD-MM<br>Fort Bliss, Texas 79916 | 1 |
| Technical Library<br>Naval Ordnance Station<br>Indian Head, Maryland 20640 | 1 |

## DISTRIBUTION (Continued)

| | No. of Copies |
|---|---|
| Commander<br>US Army Materiel Development and Readiness Command<br>ATTN: DRCMT<br>Washington, DC 20315 | 1 |
| Headquarters<br>SAC/NRI (Stinfo Library)<br>Offutt Air Force Base, Nebraska 68113 | 1 |
| Commander<br>Rock Island Arsenal<br>ATTN: SARRI-KLPL-Technical Library<br>Rock Island, Illinois 61201 | 1 |
| Commander (Code 233)<br>Naval Weapons Center<br>ATTN: Library Division<br>China Lake, California 93555 | 1 |
| Department of the Army<br>US Army Research Office<br>ATTN: Information Processing Office<br>P.O. Box 12211<br>Research Triangle Park, North Carolina 27709 | 1 |
| Commander<br>US Army Research Office<br>ATTN: DRXRO-PW, Dr. R. Lontz<br>P.O. Box 12211<br>Research Triangle Park, North Carolina 27709 | 2 |
| US Army Research and Standardization Group (Europe)<br>ATTN: DRXSN-E-RX, Dr. Alfred K. Nodoluha<br>Box 65<br>FPO New York 09510 | 2 |
| Headquarters<br>Department of the Army Office of the DCS for Research Development and Acquisition<br>Room 3A474, The Pentagon<br>ATTN: DAMA-ARZ<br>Washington, DC 20310 | 2 |

## DISTRIBUTION (Concluded)

| | No. of Copies |
|---|---|
| US Army Materiel Systems Analysis Activity<br>ATTN: DRXSY-MP<br>Aberdeen Proving Ground, Maryland 21005 | 1 |
| IIT Research Institute<br>ATTN: GACIAC<br>10 West 35th Street<br>Chicago, Illinois 60616 | 1 |
| DRSMI-LP, Mr. Voigt | 1 |
| DRSMI-R, Dr. Kobler | 1 |
| -RL, Mr. Lewis | 1 |
| -RLA, Mr. Pettey | 1 |
| Mr. Schaeffel | 50 |
| -RPR | 3 |
| -RPT (Record Set) | 1 |
| (Reference Copy) | 1 |
| -RS | 2 |
| -RSC | 2 |
| -RSP | 1 |
| -RSL | 1 |
| -RSN | 3 |
| -EAB | 1 |
| -EAT | 3 |
| -ICBB | 1 |